Published in final edited form as:

Crit Care Med. 2020 January ; 48(1): e66–e73. doi:10.1097/CCM.0000000000004073.

High-Frequency Oscillatory Ventilation and Ventilator-Induced Lung Injury: Size Does Matter

Jacob Herrmann, PhD[1,2], **Weerapong Lilitwat, MD**[3], **Merryn H. Tawhai, PhD**[4], **David W. Kaczka, MD, PhD**[1,2,5]

[1]Department of Biomedical Engineering, University of Iowa, Iowa City, IA.

[2]Department of Anesthesia, University of Iowa Hospitals and Clinics, Iowa City, IA.

[3]Department of Pediatrics, University of Iowa Hospitals and Clinics, Iowa City, IA.

[4]Auckland Bioengineering Institute, University of Auckland, Auckland, New Zealand.

[5]Department of Radiology, University of Iowa Hospitals and Clinics, Iowa City, IA.

Abstract

Objectives: The theoretical basis for minimizing tidal volume during high-frequency oscillatory ventilation may not be appropriate when lung tissue stretch occurs heterogeneously and/or rapidly. The objective of this study was to assess the extent to which increased ventilation heterogeneity may contribute to ventilator-induced lung injury during high-frequency oscillatory ventilation in adults compared with neonates on the basis of lung size, using a computational model of human lungs.

Design: Computational modeling study.

Setting: Research laboratory.

Subjects: High-fidelity, 3D computational models of human lungs, scaled to various sizes representative of neonates, children, and adults, with varying injury severity. All models were generated from one thoracic CT image of a healthy adult male.

Interventions: Oscillatory ventilation was simulated in each lung model at frequencies ranging from 0.2 to 40 Hz. Sinusoidal flow oscillations were delivered at the airway opening of each model and distributed through the lungs according to regional parenchymal mechanics.

Measurements and Main Results: Acinar flow heterogeneity was assessed by the coefficient of variation in flow magnitudes across all acini in each model. High-frequency oscillatory

For information regarding this article, david-kaczka@uiowa.edu.

Opinions, interpretations, conclusions, and recommendations are those of the authors and are not necessarily endorsed by the U.S. Department of Defense or National Institutes of Health.

Drs. Herrmann and Tawhai performed experiments. Drs. Herrmann and Kaczka prepared figures and drafted article. Drs. Herrmann, Tawhai, and Kaczka conceived and designed research; analyzed data. All authors interpreted results of experiments; edited and revised article; and approved the final version of the article.

Drs. Herrmann and Kaczka are cofounders and shareholders of OscillaVent, Inc. The remaining authors have disclosed that they do not have any potential conflicts of interest.

Supplemental digital content is available for this article. Direct URL citations appear in the printed text and are provided in the HTML and PDF versions of this article on the journal's website (http://journals.lww.com/ccmjournal).

ventilation simulations demonstrated increasing heterogeneity of regional parenchymal flow with increasing lung size, with decreasing ratio of deadspace to total acinar volume, and with increasing frequency above lung corner frequency and resonant frequency. Potential for resonant amplification was greatest in injured adult-sized lungs with higher regional quality factors indicating the presence of underdamped lung regions.

Conclusions: The potential for ventilator-induced lung injury during high-frequency oscillatory ventilation is enhanced at frequencies above lung corner frequency or resonant frequency despite reduced tidal volumes, especially in adults, due to regional amplification of heterogeneous flow. Measurements of corner frequency and resonant frequency should be considered during high-frequency oscillatory ventilation management.

Keywords

acute respiratory distress syndrome; high-frequency oscillatory ventilation; mechanical ventilation; ventilation heterogeneity; ventilator-induced lung injury

High-frequency oscillatory ventilation (HFOV) theoretically has ideal characteristics for lung-protective ventilation: low tidal volumes (V_T) that may be less than anatomic deadspace (~4 cc kg^{-1}), and mean airway pressures that may be substantially higher than positive end-expiratory pressures (PEEPs) typically applied during conventional mechanical ventilation (CMV) (1). Despite the appeal for minimizing V_T and maximizing recruitment, such strategies for HFOV have not improved mortality for acute respiratory failure in either infants or adults (2, 3). Among other factors, proposed reasons for nonsuperiority of HFOV over CMV in clinical trials include inappropriate patient selection and sub-optimal protocols for adjusting HFOV settings (4-6). By some opinions, the frequency settings used in clinical trials were not high enough to maximize the potential lung-protective benefit of V_T reduction (7, 8). Typical ranges for HFOV frequency are 4–6 Hz in adults, 6–10 Hz in children, and 10–15 Hz in neonates. However, previous experimental studies in large animals used frequencies as high as 45 Hz (9), and preliminary human studies demonstrated feasibility of frequency settings up to 15 Hz in adults (10).

In practice, the clearance of CO_2 often dictates the clinical management of HFOV settings, with delivered V_T (or pressure amplitude, ΔP) being more important than frequency in CO_2 elimination (11). Two large randomized clinical trials for treatment of the acute respiratory distress syndrome (ARDS) in adults, Oscillation in ARDS (OSCAR) and Oscillation for Acute Respiratory Distress Syndrome Treated Early (OSCILLATE), failed to show reductions in mortality compared with CMV (12, 13). As a result, enthusiasm for using HFOV in adults has waned (5, 14, 15). The OSCAR protocol prescribed initial frequency at 10 Hz, with intermittent adjustments based on arterial CO_2 tension, and with frequency adjustments secondary to adjustments of HFOV pressure amplitude (ΔP) (12). Alternatively, the OSCILLATE protocol specified a constant $\Delta P = 90$ cm H_2O, with frequency selected according to initial arterial blood pH (13). The lack of improved outcomes with HFOV has in part been attributed to hemodynamic compromise that is associated with use of increased mean airway pressure to improve lung recruitment (13).

Increasing frequency during HFOV is not without adverse physiologic consequences. Strategies to minimize V_T at the highest possible frequency are predicated upon the assumption that reduced V_T results in reduced potential for ventilator-induced lung injury (VILI) by reducing lung tissue stretch. However, it is nearly impossible to predict how oscillatory pressure and flow will be amplified or attenuated regionally throughout the lungs, based solely on inference of aggregate pressure and flow at the airway opening. Several experimental and computational investigations have associated increasing frequency with increasing heterogeneity of regional pressures and flows throughout the lung, resulting in regionally varying tissue stretch and out-of-phase oscillation (16-19). Frequency-dependent heterogeneity is especially prominent above the lung corner frequency (f_c, relating viscous to elastic forces) and resonant frequency (f_{res}, relating inertial to elastic forces) (17, 20). Furthermore, other factors influence the development and progression of VILI in addition to parenchymal strain, including strain rate (21, 22), mechanical power (23, 24), and interfacial stress in edematous lung (25, 26). HFOV has also been associated with hyperinflation and increased “auto-PEEP” (27, 28). Thus, there is potential for VILI during HFOV, despite the minimization of total delivered V_T, especially when oscillatory flows are heterogeneously distributed and subject to regional amplification or attenuation. Perceived “ideal” HFOV strategies, that minimize V_T by using the highest possible frequency to maintain eucapnia, may thus be misguided, stemming from an oversimplified understanding of lung mechanical heterogeneity and its influence on the regional propagation of VILI. Thus, HFOV presents a potentially deceptive situation, wherein seemingly protective ventilation may produce regionally injurious stresses and strains throughout the lung parenchyma.

Without presuming the relative contribution of each mechanical variable to overall injury, we conjecture that regional flow heterogeneity begets regional injury, wherever any mechanical variable is disproportionately amplified or attenuated. Considering that mortality seems to be minimally affected by ventilation modality (i.e., CMV vs HFOV), yet more strongly affected by variables homogenizing ventilation distribution (i.e., prone positioning), it is plausible that frequency-dependent ventilation heterogeneity does play a role in determining safety and efficacy of HFOV as a function of lung size. We hypothesized that lungs scaled according to neonatal and pediatric proportions would exhibit less ventilation heterogeneity compared with adult-sized lungs over typical frequency ranges used in HFOV. Although in vivo experimental measurements are impractical in adult and neonatal patients, computational modeling may provide valuable insights to address this complicated problem. In this study, we used a high-fidelity computational model of the human lung to investigate the effects of varying lung size and oscillatory frequency on the distribution of regional ventilation. Some of the results of these studies have been previously reported in the form of an abstract (29).

MATERIALS AND METHODS

Model Generation

Imaging, and subsequent use of data, was approved by the University of Iowa Institutional Review Board and Radiation Safety Committees (30). The computational model of the human lung was generated based on adult airway tree anatomy in three dimensions

(31). Central airways were segmented from a thoracic CT scan of a healthy adult male. Large airways (i.e., from the trachea to the first generation of subsegmental branches in each bronchopulmonary segment) were used as initial seeds for algorithmic generation of peripheral airways as small as 0.4 mm in diameter. The original CT image, and resulting airway network, are depicted in Figure S-1 (Supplemental Digital Content 1, http://links.lww.com/CCM/E994). Each airway segment in the model was represented by a cylinder with specified luminal diameter, length, and wall thickness. The luminal volume for each segment was specified by its cylindrical geometry. Each terminal airway of the model was subtended by a viscoelastic acinus containing a specified gas volume. Total acinar (V_A) and deadspace (V_D) volumes in the entire model were defined according to the sum of all acinar and airway luminal volumes, respectively.

The V_D and V_A of the adult-sized model were then scaled proportionally while preserving the V_D:V_A ratio of 4.4%, to obtain isometrically scaled models approximating pediatric and neonatal lungs. One additional model was created with an altered V_D:V_A ratio of 6.0%, to better represent neonatal anatomy with comparatively similar deadspace per unit body weight (32) yet immature alveolarization (33). Airway segments were scaled isometrically to achieve the specified V_D, while preserving diameter-to-length ratios and branching angles. Acinar volumes were distributed according to a spatial distribution of acinar tissue viscoelasticity, which was assumed to vary according to a quadratic function of time-averaged transpulmonary pressure (34). Transpulmonary pressure was defined as the difference between mean airway pressure and local pleural pressure, which was assumed to vary linearly in the gravitational field with mean −5 cm H_2O and a vertical gradient of 0.25 cm H_2O cm^{-1} (35). Mean airway pressure was set to 10 cm H_2O for all simulations.

Simulations

Frequency-dependent relationships between pressure and flow across the model elements have been detailed elsewhere (16, 36). Briefly, each airway segment and terminal acinus was modeled with an arrangement of series and parallel mechanical impedances (Fig. S-1, Supplemental Digital Content 1, http://links.lww.com/CCM/E994). Each airway segment accounted for resistive and inertial pressure losses, as well as gas compression and viscoelastic wall distension.

Each acinus was characterized by tissue hysteresivity, tissue elastance, and gas compression. Oscillatory flow was distributed throughout the model according to a recursive flow division algorithm, based on the mechanical impedance of series and parallel branches in the network (36). Flow at each node of the network was apportioned to subtending branches in inverse proportion to the total input impedance of each subtending branch. Flow throughout the model was described by real (in phase with pressure) and imaginary (out of phase with pressure) components, ensuring conservation of mass such that the sum of complex-valued flow across all gas compression and wall distension pathways was equal to the total flow delivered to the airway opening (16). Since the flow distribution was based on regional transpulmonary pressure gradients, the simulations made no assumptions regarding chest wall impedance.

Lung injury was simulated using a heterogeneous pseudorandom distribution of tissue elastances, to mimic alveolar flooding and surfactant dysfunction, with gravitational weighting to impose increased parenchymal stiffness in the dependent region of the model, assuming supine position (17). Derecruitment was imposed in according to a tissue stiffness threshold (37). Increasing injury severity was modeled by increasing injured tissue elastances, corresponding to 10% (mild), 25% (moderate), and 50% (severe) acinar derecruitment. In addition to a single healthy condition at each lung size, 10 randomized spatial patterns of injury were generated at each lung size and level of injury.

Simulated oscillatory ventilation was then applied by imposing sinusoidal variations in tracheal flow, and computing the resulting distribution of oscillatory flows at each node of the model. Two-hundred frequencies, spanning 0.2–40 Hz (12–2,400 min^{-1}), were simulated for models ranging in size from 2% to 100% of that of an adult lung. Acinar flow magnitudes for each simulation were normalized by the total flow amplitude at the airway opening, such that a normalized acinar flow magnitude equal to 1 corresponds to what would be obtained for a completely homogeneous distribution of delivered flow (i.e., in a symmetrically branching tree with rigid airway walls and no gas compression). Thus, acinar flows above and below 1 correspond to relative over- and under-ventilation, respectively. The heterogeneity of acinar flow was then assessed by its coefficient of variation across all acini. Corner frequency f_c was estimated using lung resistance at 40 Hz and lung compliance at 0.2 Hz, according to the formula of Venegas and Fredberg (20). Resonant frequency f_{res} was determined from the zero-crossing of the imaginary part of the impedance spectrum (16). The quality factor q was estimated as the ratio of f_c to f_{res}, characterizing the mechanical response as overdamped for $q < 1$ and underdamped for $q > 1$ (20). A summary of the physical meanings for f_c, f_{res}, and q in the context of respiratory mechanics is provided in the Discussion.

RESULTS

Figure 1 shows representative examples of simulation results for lung sizes scaled to a few selected values of V_D and V_A. All lung sizes exhibit varying degrees of heterogeneity in normalized acinar flow magnitude, with distinct regions of relative amplification and attenuation. These regions were spatially clustered, indicating that flow distribution during HFOV exhibits strong dependence on the inertial properties of the airways, with diminishing influence of regional tissue elastance.

Isometric scaling from adult size to neonatal size, with preserved V_D:V_A ratio, demonstrated reductions in ventilation heterogeneity, as indicated by the coefficient of variation of acinar flow. Comparing 4% to 100% of adult size, flow heterogeneity was reduced by 14% at 5 Hz and 24% at 10 Hz. The neonatal lung size, with altered V_D:V_A ratio, demonstrated further reductions in acinar flow heterogeneity: 26% at 5 Hz and 32% at 10 Hz. Increasing frequency from 5 to 10 Hz resulted in increased flow heterogeneity by 32% to 49%, depending on lung size.

Figure 2 shows characteristics of the acinar flow distribution in the recruited lung as a function of lung size for selected frequencies. Both acinar flow mean and SD increase with

injury severity, due to increasing tissue elastance heterogeneity and derecruitment. Increased normalized flow mean in injured lungs indicates the disproportionate burden of the recruited lung regions, compensating for zero flow in the derecruited acini. Acinar flow heterogeneity also increased in larger lungs, especially at higher frequencies. Lungs scaled to neonatal proportions consistently exhibited less acinar flow heterogeneity compared with similarly sized lungs scaled isometrically from the adult lung. However, this effect size was small compared with the variability in flow heterogeneity associated with injury severity.

Figure 3 shows lobar segmental flow distributions as a function of frequency with respect to segmental f_c, f_{res}, and q for an example healthy adult lung model. Segmental flow heterogeneity at high frequencies was associated with variations in segmental f_c, f_{res}, and q, such that regions with higher values of f_c, f_{res}, or q tended to exhibit flow amplification at high frequencies, while regions with lower values tended to exhibit flow attenuation. For this healthy condition, all values of segmental f_c were smaller than the corresponding f_{res}, and thus all values of segmental q were less than unity.

Figure 4A shows acinar flow heterogeneity as a function of frequency for selected lung sizes, indicating reduced heterogeneity in smaller lungs across the entire range of frequencies less than 40 Hz. The effect of lung size on acinar flow heterogeneity is especially prominent for frequencies above 6 Hz. Figure 4, B and C, show the same data with oscillation frequency normalized by f_{res} and f_c, respectively. Normalization by f_c provided the best marker of the onset of frequency-dependent flow heterogeneity with increasing frequency. Values of f_c and f_{res} decrease as lung size increases but increase with increasing injury severity (Fig. S-2, Supplemental Digital Content 1, http://links.lww.com/CCM/E994). Other global lung mechanical measurements, including airways resistance, airways inertance, tissue hysteresivity, and tissue elastance are provided as well for the healthy condition (Table S-1 and Fig. S-3, Supplemental Digital Content 1, http://links.lww.com/CCM/E994).

None of the conditions, for any size or severity of injury, exhibited total lung underdamping as would be indicated by $q > 1$ (Fig. S-2, Supplemental Digital Content 1, http://links.lww.com/CCM/E994). However, there was interregional variability in q across individual lobar segments, as shown in Figure 5. Although the healthy condition exhibited no segmental underdamping regardless of size, larger lung sizes, and more severe lung injury were associated with a greater likelihood of one or more underdamped lobar segments, with $q > 1$.

DISCUSSION

This study of distributed oscillatory flow in a high-fidelity computational model of a human lung revealed two primary findings are as follows: 1) smaller lung size is associated with reduced heterogeneity of parenchymal oscillatory flow magnitude at all frequencies and 2) increasing frequency is associated with increasing flow heterogeneity, especially in larger lung sizes at frequencies above the corner frequency or resonant frequency (whichever is smaller). These findings support the notion that HFOV may be less injurious in neonates compared with adults, over the range of frequencies typically used in clinical settings. More

importantly, these findings promote caution with regard to setting frequency at extremely high rates. The benefit gained from V_T reduction may be outweighed by the detriment associated with increased ventilation heterogeneity. As our simulations demonstrate, there may be an optimal combination of f and ΔP for a particular patient, such that exceeding the optimal values for either parameter might unintentionally increase risk for regional lung injury. This hypothesis is speculative, although based on simulations (16, 17, 36) and experimental data (18, 19, 38), there is support for measurement of global respiratory mechanics to guide HFOV management (20, 39, 40).

Our characterization of the lungs' mechanical frequency response involves several key engineering terms that are briefly described here. The corner frequency f_c and resonant frequency f_{res} delineate frequency ranges over which different mechanical factors (i.e., resistance, elastance, inertance) dominate the behavior of gas flows. Although f_c is typically used to describe transitional frequencies in filters, the lung as a whole may be considered a "low-pass" filter. That is, low-frequency ($f < f_c$) pressure oscillations are "passed" from the airway opening to the alveolar spaces, while high-frequency ($f > f_c$) pressure oscillations are heavily attenuated by resistive losses. Resonance describes a maximum transfer of oscillating pressure energy between elastically distending tissue and inertially accelerating gas, occurring when the mechanical impedance contributions of elastance and inertance are equal and opposite. Elastance contributes more to impedance for $f < f_{res}$, and inertance more for $f > f_{res}$. The quality factor q, defined as the ratio of f_c to f_{res}, relates resistance to the product of elastance and inertance. Thus, q characterizes the overall behavior as underdamped ($q > 1$, rapid response to sudden changes and resonant amplification) or overdamped ($q < 1$, slow response to sudden changes and unforced oscillations quickly decay).

In the lungs, flow heterogeneity at any particular frequency may be largely determined by the relative contributions of resistive, elastic, and inertial factors. For example in otherwise healthy lungs with homogeneous tissue elastance, there may be heterogeneity of airway resistance and inertance due to asymmetrical branching, nonuniform airway lengths and diameters, and nonuniform path lengths from the trachea to the acini. However, homogeneous tissue elastance dominates mechanical impedance at frequencies below f_c and f_{res}, and the lungs inflate homogeneously. At frequencies above f_c or f_{res} (whichever is smaller), regional differences in mechanical impedance will produce regional heterogeneity of distributed flow.

Increasing injury severity was associated with increased lung f_c and f_{res}, such that the onset of frequency-dependent flow heterogeneity occurred at a higher oscillation frequency in more severely injured lungs. This finding suggests that higher frequencies during HFOV may be beneficial for patients with more severe injury, which is typically associated with derecruitment reduced lung compliance. This may in part explain why HFOV is associated with lower mortality in patients with severe hypoxemia (41). HFOV resulted in greater frequency-dependence of flow heterogeneity at lower frequencies in the healthy condition compared with the injured conditions. However, the overall degree of flow heterogeneity during injury was much greater than that for the healthy condition at all frequencies below 5 Hz. Thus, the underlying mechanical heterogeneity in the recruited lung regions

may determine the baseline degree of flow heterogeneity at low frequencies, while the lung compliance and recruitment may determine the onset and relative increase of flow heterogeneity at higher frequencies.

Although other HFOV parameters such as mean airway pressure, bias flow, and inspiratory time were not included in our analysis, their exclusion by no means implies a lack of influence on outcomes associated with HFOV use (42). The purpose of this study was not to identify mechanisms by which HFOV failed in clinical trials, but rather to probe the effects and interactions of frequency and lung size on ventilation heterogeneity. Our findings support consideration of frequency limitation during HFOV management, especially for mild-to-moderate degrees of lung injury. Furthermore, intermittent measurements of f_c and f_{res} may also guide frequency settings, especially for adult patients or for frequencies beyond the recommended ranges. An optimal balance between V_T reduction and ventilation heterogeneity might be achieved by setting the oscillator frequency to f_c or f_{res}, whichever is smaller. These settings should be based on lung mechanics measured as close as possible to the carina, since the trachea and endotracheal tube supply large resistive and inertial contributions. Further validation of such assumptions may require investigation of the relative contributions of strain, strain rate, or mechanical power to VILI during HFOV.

Other recommendations are based on the pressure cost of ventilation, that is: minimizing the extremes of pressure transmitted to the carina (20, 43). In overdamped lungs, this approach also minimizes the extremes of pressure transmitted to the parenchymal tissues. The pressure cost increases with $f > f_c$, especially in overdamped lungs, with potential for tissue damage (20). Although the optimal frequency obtained by this method is often near f_c or f_{res} (whichever is smaller), the conceptual basis for minimizing the pressure cost of HFOV does not consider the impact of mechanical heterogeneity (20). Such heterogeneity is a typical feature of lung injury (44, 45), and therefore presents a critical limitation of these heuristics in HFOV management. Injurious regional deformations may occur throughout the lung despite seemingly “safe” oscillatory pressure amplitudes at the carina, particularly in underdamped lungs or lung regions. It is worth noting that distal resonant amplification depends on the quality factor ($q > 1$), and is therefore less likely to occur in neonatal lungs compared with adult lungs. In this study, although q increased after simulated injury, there was no case in which q for the entire lung was greater than unity (Fig. S-2, Supplemental Digital Content 1, http://links.lww.com/CCM/E994). Nevertheless, there was greatly increased regional q in different lobar segments (Fig. 5).

The mechanism by which increased ventilation heterogeneity contributes to VILI might in part account for the perceived discrepancy between outcomes associated with HFOV in neonatal and pediatric populations as compared with adults. In our simulations, reductions in flow heterogeneity associated with reduced lung size were enhanced by scaling the total acinar and deadspace volumes according to values typical for neonates, as opposed to just isometric scaling with adult proportions. This finding highlights the importance of the V_D:V_A ratio as a determinant of the relative resistive, elastic, and inertial components of lung mechanics, and thus as a potential predictor of frequency-dependent ventilation heterogeneity. In addition to lung size, developmental variations in the relative sizes of airways and acini may also partly explain perceived differences in HFOV efficacy in

neonates compared with adults (46). However, the influence of developmental age and physiologic maturity on susceptibility to VILI is not fully understood (47). Differences in lung anatomy, size, and mechanical properties may contribute to differences in f_c and f_{res} and frequency-dependent ventilation distribution. For example, values of f_{res} in neonatal lungs are typically 12–24 Hz (43, 48), as compared with 6–8 Hz in normal adults (49). As a result, HFOV at an arbitrary frequency of 10 Hz, for example, may be more protective in neonates than in adults, due to differences in regional lung stress and strain distributions.

Recommended initial frequency settings for adults (5–6 Hz), children (6–10 Hz), and neonates (10–15 Hz) are at or below typical values for resonance in healthy lungs for each respective patient population. However, f_c is typically less than f_{res}, such that healthy lungs may be exposed to relatively increased flow heterogeneity at these rates. By contrast, the most severe injury model in this study exhibited corner frequencies consistent with these initial frequency ranges. Protocolizing initial frequency settings on the basis of body weight may therefore be a reasonable approach in the absence of f_c and f_{res} measurement, especially in neonates (50). However, various pathologies may alter lung mechanics in ways that affect f_c and f_{res} —generally, the ARDS is accompanied by reductions in compliance and increases in f_c and f_{res} (45). Nevertheless, there is plausible concern that arbitrary selection of high frequencies may present greater risk for heterogeneous regional amplification of flow.

There are several important limitations to consider when interpreting our simulations. The computational model presented here is based on the anatomy of a single subject and assumed a relatively healthy distribution of airway mechanical properties. The model does not account for more complicated factors such as parenchymal interdependence, mechanical nonlinearity, intratidal variations in airway and acinar dimensions, or influences from the chest wall. Although the branching structure of neonatal airways is fully developed at birth (32), further structural variations associated with lung development (e.g., alveolarization) were not specifically modeled (33). These factors may contribute additional influence on the particular distribution of oscillatory flows in the lung. For example, viscous coupling between the lung and chest wall may result in altered spatial distributions of flow and potentially reduced flow heterogeneity at high frequencies (51). Nevertheless, the overall degree of ventilation heterogeneity predicted by a computational model using a canine airway network is consistent with experimental measurements of regional parenchymal pressure and strain (52). We therefore expect these simulations to be physiologically relevant, if not spatially predictive.

CONCLUSIONS

Our simulations of HFOV in branching airway networks revealed increasing heterogeneity of parenchymal distension with increasing lung size, with decreasing ratio of deadspace to total acinar volume, and with increasing oscillation frequency above lung corner frequency or resonant frequency. Heterogeneous parenchymal distension during HFOV may intensify VILI despite reduced total V_{TS}, especially in regions exposed to amplified strain, strain rate, and mechanical power. These findings may in part explain discrepancies in HFOV outcomes in neonates and children compared with adults. Furthermore, these findings demonstrate the importance of considering other patient lung characteristics (e.g., corner frequency, resonant

frequency, or quality factor) when selecting appropriate HFOV frequencies, as opposed to arbitrary settings based solely on gas exchange.

Supplementary Material

Refer to Web version on PubMed Central for supplementary material.

Acknowledgments

Supported, in part, by grant from the Office of the Assistant Secretary of Defense for Health Affairs through the Peer Reviewed Medical Research Program under Award number W81XWH-16-1-0434, the University of Iowa Hospitals and Clinics Department of Anesthesia, the National Heart, Lung, and Blood Institute Grants R01-HL-112986 and R01-HL-126838, and the University of Auckland Medical Technologies Centre of Research Excellence.

REFERENCES

1. Pillow JJ: High-frequency oscillatory ventilation: Mechanisms of gas exchange and lung mechanics. Crit Care Med 2005; 33:S135–S141 [PubMed: 15753719]
2. Cools F, Offringa M, Askie LM: Elective high frequency oscillatory ventilation versus conventional ventilation for acute pulmonary dysfunction in preterm infants. Cochrane Database Syst Rev 2015; (3):CD000104 [PubMed: 25785789]
3. Sud S, Sud M, Friedrich JO, et al. : High-frequency oscillatory ventilation versus conventional ventilation for acute respiratory distress syndrome. Cochrane Database Syst Rev 2016; 4:CD004085 [PubMed: 27043185]
4. Sklar MC, Fan E, Goligher EC: High-frequency oscillatory ventilation in adults with ARDS: Past, present, and future. Chest 2017; 152:1306–1317 [PubMed: 28684287]
5. Malhotra A, Drazen JM: High-frequency oscillatory ventilation on shaky ground. N Engl J Med 2013; 368:863–865 [PubMed: 23339640]
6. Dreyfuss D, Ricard JD, Gaudry S: Did studies on HFOV fail to improve ARDS survival because they did not decrease VILI? On the potential validity of a physiological concept enounced several decades ago. Intensive Care Med 2015; 41:2076–2086 [PubMed: 26438222]
7. Kneyber MC, Markhorst DG: Do we really know how to use high-frequency oscillatory ventilation in critically ill children? Am J Respir Crit Care Med 2016; 193:1067–1068 [PubMed: 27128708]
8. Fessler HE, Derdak S, Ferguson ND, et al. : A protocol for high-frequency oscillatory ventilation in adults: Results from a roundtable discussion. Crit Care Med 2007; 35:1649–1654 [PubMed: 17522576]
9. Lunkenheimer PP, Redmann K, Stroh N, et al. : High-frequency oscillation in an adult porcine model. Crit Care Med 1994; 22:S37–S48 [PubMed: 8070269]
10. Fessler HE, Hager DN, Brower RG: Feasibility of very high-frequency ventilation in adults with acute respiratory distress syndrome. Crit Care Med 2008; 36:1043–1048 [PubMed: 18379227]
11. Venegas JG, Hales CA, Strieder DJ: A general dimensionless equation of gas transport by high-frequency ventilation. J Appl Physiol (1985) 1986; 60:1025–1030 [PubMed: 3082848]
12. Young D, Lamb SE, Shah S, et al. ; OSCAR Study Group: High-frequency oscillation for acute respiratory distress syndrome. N Engl J Med 2013; 368:806–813 [PubMed: 23339638]
13. Ferguson ND, Cook DJ, Guyatt GH, et al. ; OSCILLATE Trial Investigators; Canadian Critical Care Trials Group: High-frequency oscillation in early acute respiratory distress syndrome. N Engl J Med 2013; 368:795–805 [PubMed: 23339639]
14. Vincent JL: High-frequency oscillation in acute respiratory distress syndrome. The end of the story? Am J Respir Crit Care Med 2017; 196:670–671 [PubMed: 28914571]
15. Adhikari NK, Slutsky AS: Pediatric high-frequency oscillation. The end of the road? Am J Respir Crit Care Med 2016; 193:471–472 [PubMed: 26930425]

16. Amini R, Kaczka DW: Impact of ventilation frequency and parenchymal stiffness on flow and pressure distribution in a canine lung model. Ann Biomed Eng 2013; 41:2699–2711 [PubMed: 23872936]
17. Herrmann J, Tawhai MH, Kaczka DW: Regional gas transport in the heterogeneous lung during oscillatory ventilation. J Appl Physiol (1985) 2016; 121:1306–1318 [PubMed: 27763872]
18. Lehr JL, Butler JP, Westerman PA, et al. : Photographic measurement of pleural surface motion during lung oscillation. J Appl Physiol (1985) 1985; 59:623–633 [PubMed: 4030616]
19. Fredberg JJ, Keefe DH, Glass GM, et al. : Alveolar pressure nonhomogeneity during small-amplitude high-frequency oscillation. J Appl Physiol Respir Environ Exerc Physiol 1984; 57:788–800 [PubMed: 6490465]
20. Venegas JG, Fredberg JJ: Understanding the pressure cost of ventilation: Why does high-frequency ventilation work? Crit Care Med 1994; 22:S49–S57 [PubMed: 8070270]
21. Protti A, Maraffi T, Milesi M, et al. : Role of strain rate in the pathogenesis of ventilator-induced lung edema. Crit Care Med 2016; 44:e838–e845 [PubMed: 27054894]
22. Cooper GJ, Taylor DE: Biophysics of impact injury to the chest and abdomen. J R Army Med Corps 1989; 135:58–67 [PubMed: 2527980]
23. Gattinoni L, Tonetti T, Cressoni M, et al. : Ventilator-related causes of lung injury: The mechanical power. Intensive Care Med 2016; 42:1567–1575 [PubMed: 27620287]
24. Cressoni M, Gotti M, Chiurazzi C, et al. : Mechanical power and development of ventilator-induced lung injury. Anesthesiology 2016; 124:1100–1108 [PubMed: 26872367]
25. Hussein O, Walters B, Stroetz R, et al. : Biophysical determinants of alveolar epithelial plasma membrane wounding associated with mechanical ventilation. Am J Physiol Lung Cell Mol Physiol 2013; 305:L478–L484 [PubMed: 23997173]
26. Hamlington KL, Smith BJ, Dunn CM, et al. : Linking lung function to structural damage of alveolar epithelium in ventilator-induced lung injury. Respir Physiol Neurobiol 2018; 255:22–29 [PubMed: 29742448]
27. Simon BA, Weinmann GG, Mitzner W: Mean airway pressure and alveolar pressure during high-frequency ventilation. J Appl Physiol Respir Environ Exerc Physiol 1984; 57:1069–1078 [PubMed: 6501027]
28. Cha EJ, Chow E, Chang HK, et al. : Lung hyperinflation in isolated dog lungs during high-frequency oscillation. J Appl Physiol (1985) 1988; 65:1172–1179 [PubMed: 3182488]
29. Herrmann J, Tawhai MH, Kaczka DW: Lung size and ventilation heterogeneity: A comparison of high-frequency oscillatory ventilation in neonates and adults. Am J Respir Crit Care Med 2018; 197:A4663
30. Hedges KL, Clark AR, Tawhai MH: Comparison of generic and subject-specific models for simulation of pulmonary perfusion and forced expiration. Interface Focus 2015; 5:20140090 [PubMed: 25844154]
31. Tawhai MH, Hunter P, Tschirren J, et al. : CT-based geometry analysis and finite element models of the human and ovine bronchial tree. J Appl Physiol (1985) 2004; 97:2310–2321 [PubMed: 15322064]
32. Pinkerton KE, Herring MJ, Hyde DM, et al.: Normal aging of the lung. *In*: The Lung. Harding R, Pinkerton KE (Eds). London, Elsevier, 2014, pp 265–285
33. Schittny JC: Development of the lung. Cell Tissue Res 2017; 367:427–444 [PubMed: 28144783]
34. Kaczka DW, Smallwood JL: Constant-phase descriptions of canine lung, chest wall, and total respiratory system viscoelasticity: Effects of distending pressure. Respir Physiol Neurobiol 2012; 183:75–84 [PubMed: 22691447]
35. Lai-Fook SJ, Rodarte JR: Pleural pressure distribution and its relationship to lung volume and interstitial pressure. J Appl Physiol (1985) 1991; 70:967–978 [PubMed: 2033012]
36. Colletti AA, Amini R, Kaczka DW: Simulating ventilation distribution in heterogenous lung injury using a binary tree data structure. Comput Biol Med 2011; 41:936–945 [PubMed: 21872852]
37. Herrmann J, Tawhai MH, Kaczka DW: Computational modeling of primary blast lung injury: Implications for ventilator management. Mil Med 2019; 184:273–281 [PubMed: 30901433]

38. Allen JL, Fredberg JJ, Keefe DH, et al. : Alveolar pressure magnitude and asynchrony during high-frequency oscillations of excised rabbit lungs. Am Rev Respir Dis 1985; 132:343–349 [PubMed: 4026057]
39. Dellacà RL, Zannin E, Ventura ML, et al. : Assessment of dynamic mechanical properties of the respiratory system during high-frequency oscillatory ventilation*. Crit Care Med 2013; 41:2502–2511 [PubMed: 23760105]
40. Zannin E, Ventura ML, Dellacà RL, et al. : Optimal mean airway pressure during high-frequency oscillatory ventilation determined by measurement of respiratory system reactance. Pediatr Res 2014; 75:493–499 [PubMed: 24375086]
41. Meade MO, Young D, Hanna S, et al. : Severity of hypoxemia and effect of high-frequency oscillatory ventilation in acute respiratory distress syndrome. Am J Respir Crit Care Med 2017; 196:727–733 [PubMed: 28245137]
42. Guervilly C, Forel JM, Hraiech S, et al. : Right ventricular function during high-frequency oscillatory ventilation in adults with acute respiratory distress syndrome. Crit Care Med 2012; 40:1539–1545 [PubMed: 22511135]
43. Zannin E, Dellaca' RL, Dognini G, et al. : Effect of frequency on pressure cost of ventilation and gas exchange in newborns receiving high-frequency oscillatory ventilation. Pediatr Res 2017; 82:994–999 [PubMed: 28665929]
44. Kaczka DW, Cao K, Christensen GE, et al. : Analysis of regional mechanics in canine lung injury using forced oscillations and 3D image registration. Ann Biomed Eng 2011; 39:1112–1124 [PubMed: 21132371]
45. Kaczka DW, Hager DN, Hawley ML, et al. : Quantifying mechanical heterogeneity in canine acute lung injury: Impact of mean airway pressure. Anesthesiology 2005; 103:306–317 [PubMed: 16052113]
46. Nguyen AP, Schmidt UH, MacIntyre NR: Should high-frequency ventilation in the adult be abandoned? Respir Care 2016; 61:791–800 [PubMed: 27235314]
47. Kneyber MC, Zhang H, Slutsky AS: Ventilator-induced lung injury. Similarity and differences between children and adults. Am J Respir Crit Care Med 2014; 190:258–265 [PubMed: 25003705]
48. Lee S, Alexander J, Blowes R, et al. : Determination of resonance frequency of the respiratory system in respiratory distress syndrome. Arch Dis Child Fetal Neonatal Ed 1999; 80:F198–202 [PubMed: 10212081]
49. Bates JH, Irvin CG, Farré R, et al. : Oscillation mechanics of the respiratory system. Compr Physiol 2011; 1:1233–1272 [PubMed: 23733641]
50. Kneyber MC, van Heerde M, Markhorst DG: Reflections on pediatric high-frequency oscillatory ventilation from a physiologic perspective. Respir Care 2012; 57:1496–1504 [PubMed: 22348243]
51. Venegas JG, Tsuzaki K, Fox BJ, et al. : Regional coupling between chest wall and lung expansion during HFV: A positron imaging study. J Appl Physiol (1985) 1993; 74:2242–2252 [PubMed: 8335554]
52. Herrmann J, Tawhai MH, Kaczka DW: Parenchymal strain heterogeneity during oscillatory ventilation: Why two frequencies are better than one. J Appl Physiol (1985) 2018; 124:653–663 [PubMed: 29051332]

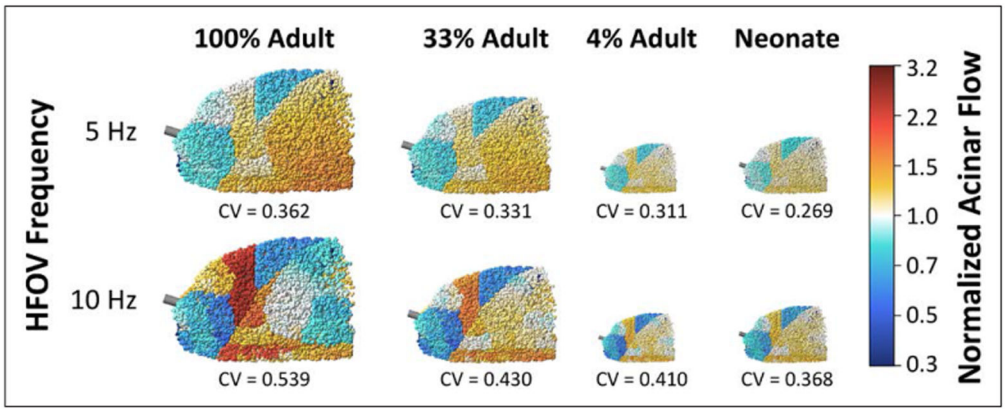

Figure 1.

Spatial distributions of normalized acinar flow in selected healthy lung models, using either neonatal proportions of deadspace and total acinar volume, or isometrically scaled down versions of the adult lung model. Normalized acinar flows above or below 1 represent relative over- or under-ventilation, respectively. Regional heterogeneity was assessed by the coefficient of variation (CV) across all acini. HFOV = high-frequency oscillatory ventilation.

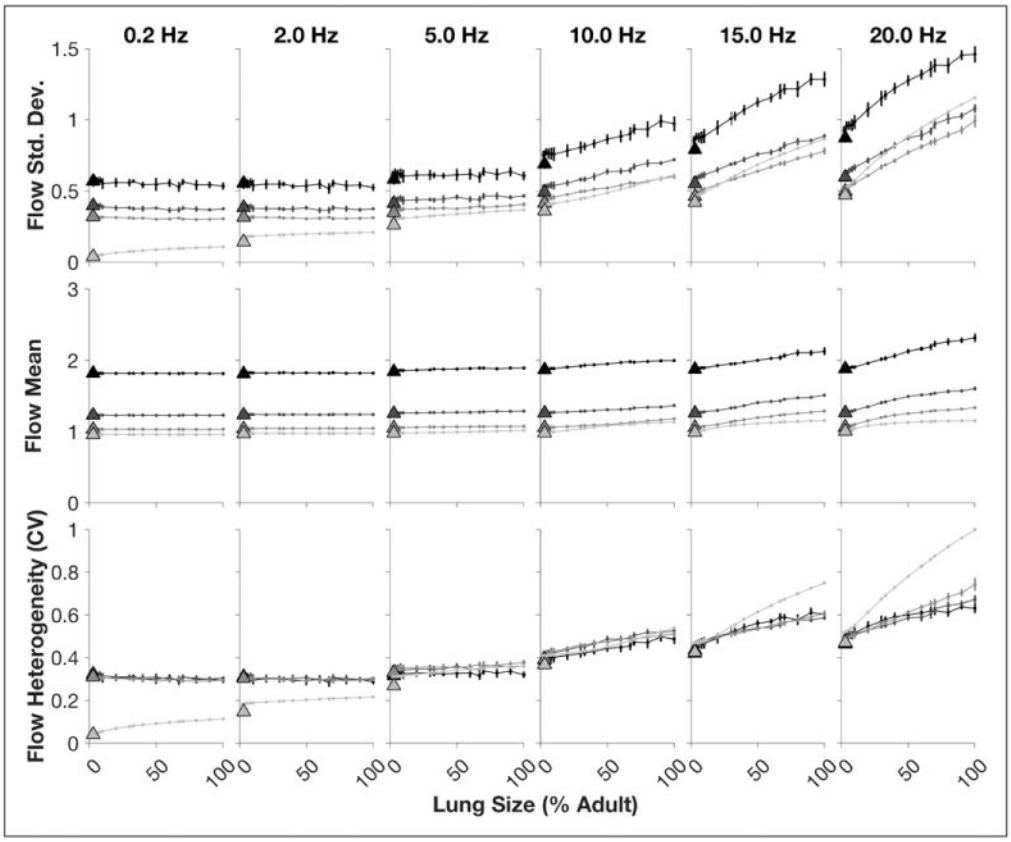

Figure 2.

Acinar flow distribution characteristics in the recruited regions of the lung model during oscillation at selected frequencies between 0.2 Hz and 20 Hz. Increasing injury severity, modeled by randomized spatial patterns of heterogeneous tissue elastance and derecruitment, is shown for the healthy condition (*light gray*) to severe injury (*black*). *Error bars* denote SD from 10 random spatial patterns of lung tissue stiffness and derecruitment. *Points* connected by *lines* represent isometrically scaled lungs (relative to the adult model). *Triangles* represent lungs scaled to neonatal proportions. CV = coefficient of variation.

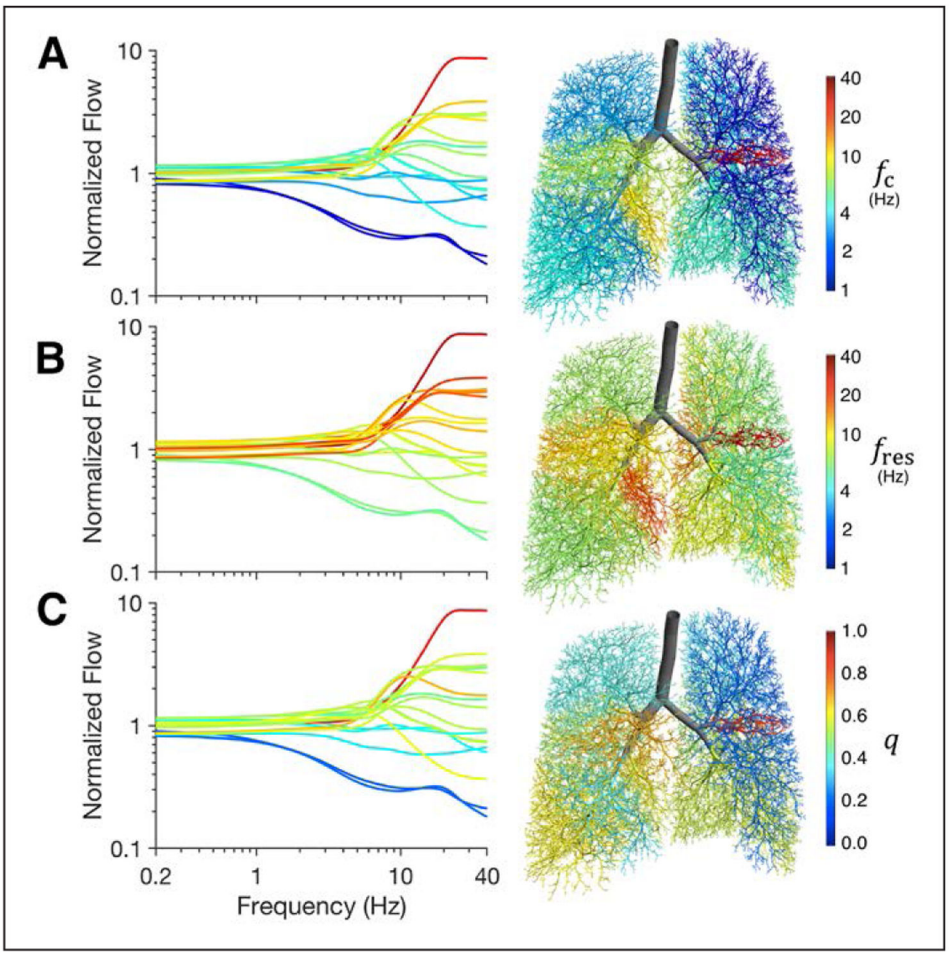

Figure 3.

Lobar segmental flow distributions, normalized by lobar segmental volumes, for a healthy adult lung model, demonstrating increasing segmental flow heterogeneity with increasing frequency. *Lines* and *airways* are colored according to corresponding segmental values of: corner frequency (**A**), resonant frequency (**B**), or quality factor (**C**). The corner and resonant frequencies for the entire lung model in this example were 2.8 Hz and 4.7 Hz, respectively. The overall quality factor was 0.60. f_c = corner frequency, f_{res} = resonant frequency, q = quality factor.

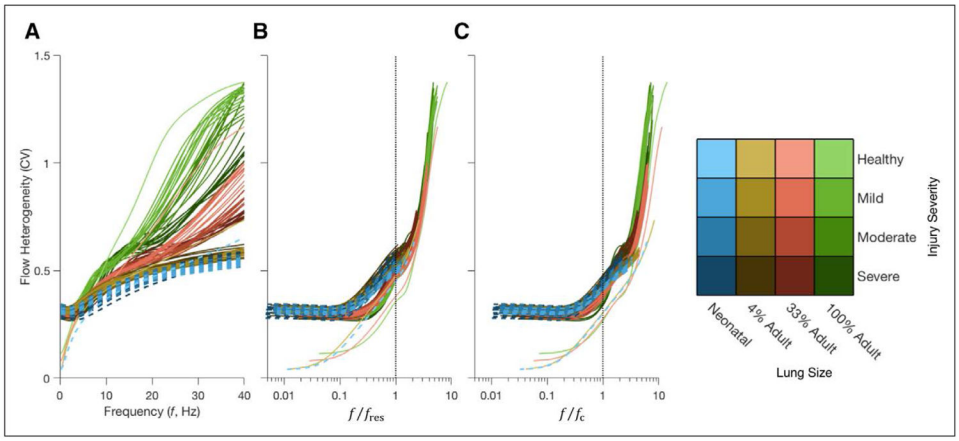

Figure 4.

Flow heterogeneity in the lung model as a function of: oscillation frequency in Hz (**A**), as well as oscillation frequency normalized by either the lung resonant frequency (**B**) or lung corner frequency (**C**). *Color hue* indicates lung size, while *color intensity* represents injury severity. *Dashed lines* indicate the flow heterogeneity for the model as scaled to neonatal proportions. CV = coefficient of variation, f = frequency, f_c = corner frequency, f_{res} = resonant frequency.

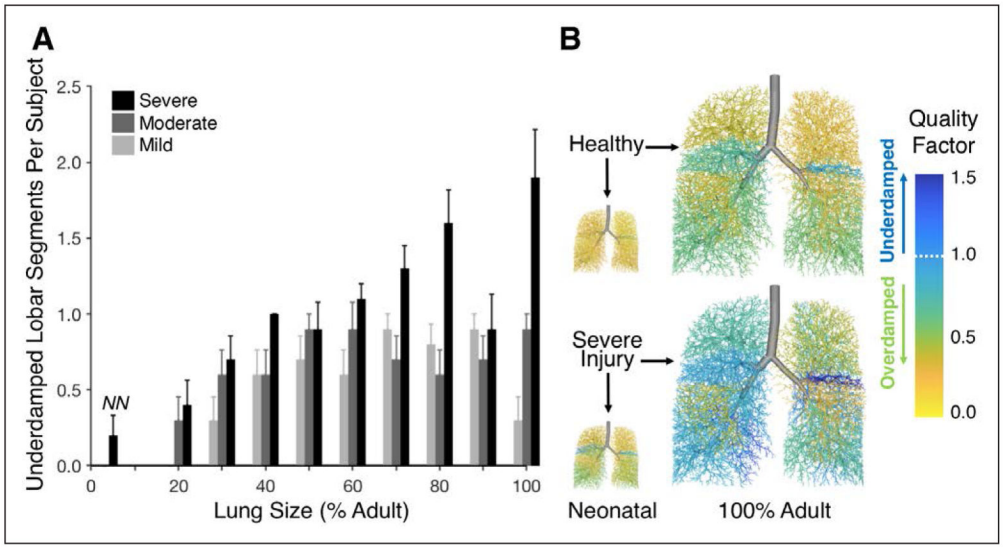

Figure 5.

Quality factor q in lobar segments. **A**, Mean and SE for the number of underdamped segments ($q > 1$) across varying lung size, with 10 random spatial patterns of lung tissue stiffness and derecruitment at each severity level from mild to severe (*light gray* to *black*). No underdamped segments were found in healthy models, nor at any injury severity in isometrically scaled models below 20% adult size. The models scaled to neonatal proportions of deadspace to acinar volume are indicated by "*NN*." **B**, Representative airway trees with airways colored according to segmental quality factor.